iScience

CellPress
OPEN ACCESS

Article

Notch signaling generates the "cut here line" on the cuticle of the puparium in *Drosophila melanogaster*

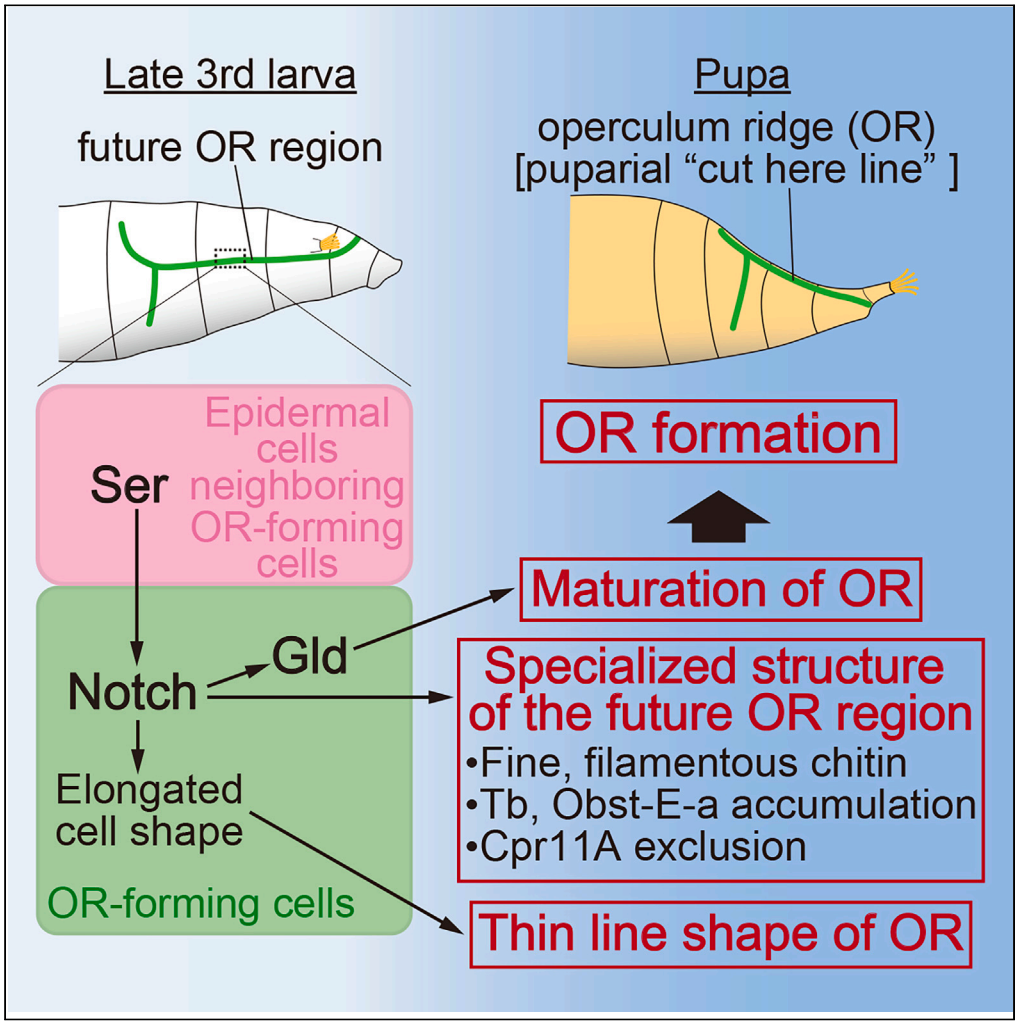

Reiko Tajiri, Ayaka Hirano, Yu-ya Kaibara, Daiki Tezuka, Zhengyang Chen, Tetsuya Kojima

tkojima@k.u-tokyo.ac.jp

Highlights

Notch signaling in OR-forming cells activated by Ser is required for OR formation

Unique structure formation at the future OR region requires Notch signaling

Gld activation by Notch signaling is required for OR maturation in the pupal stage

Elongated OR-forming cell shape is regulated by Notch signaling

Tajiri et al., iScience *26*, 107279
August 18, 2023
https://doi.org/10.1016/j.isci.2023.107279

iScience

CellPress
OPEN ACCESS

Article

Notch signaling generates the "cut here line" on the cuticle of the puparium in *Drosophila melanogaster*

Reiko Tajiri,[1,2] Ayaka Hirano,[1] Yu-ya Kaibara,[1] Daiki Tezuka,[1] Zhengyang Chen,[1] and Tetsuya Kojima[1,3,*]

SUMMARY

During a molt or eclosion, insects shed their cuticle, an extracellular matrix made by underlying epidermal cells, by cleavage along a defined line. This means that the "cut here line" is pre-formed on the cuticle, and its formation is indispensable for insect life. Here, we show that the proper formation of the operculum ridge (OR), which is the "cut here line" on the puparium (pupal case) of *Drosophila melanogaster*, involves Notch signaling activation in the epidermal cells just beneath the future OR region (OR-forming cells). The inhibition of Notch signaling causes defects in eclosion due to failure in OR cleavage, the chitin organization and several cuticular proteins localization, glucose dehydrogenase (Gld) activity, and OR-forming cell shape. Our findings provide the first insight into the molecular basis of the structure and formation of the "cut here line" on the cuticle.

INTRODUCTION

One of the characteristic features of arthropods, including insects, is that their surfaces are covered by a cuticle, which is made of materials secreted by the underlying epidermal cells. The insect cuticle is largely divided into three layers. The outermost layer is the lipophilic envelope. Underneath the envelope is the epicuticle, which is mainly formed by proteins. The innermost layer is the procuticle, and it contains chitin (a polymer of *N*-acetylglucosamine) and proteins. In many cases, the procuticle is further subdivided into two layers: an outer layer called the exocuticle, which is sclerotized and colored, and an inner layer called the endocuticle, which is colorless and relatively soft.[1,2] The cuticle has a rigid property and functions as an exoskeleton and a protective barrier against the environment. Recent studies have shown that the cuticle is also involved in controlling the body shape.[3–9] Because the expandability of the cuticle is limited by its rigidity, it is necessary to produce a new cuticle and shed the old cuticle during molt for larval growth and eclosion for emergence of adults. In these processes, the old cuticle is not broken randomly but is cleaved along a defined line. This means that some kind of a "cut here line" is pre-formed during cuticle formation. This cleavage site on the cuticle has also been referred to as the "ecdysial line," "ecdysial suture," or "line of weakness." Although the "cut here line" on the cuticle is important for the molt and eclosion, and thus, critical for development and survival, its ultrastructure, composition, and mechanisms underlying its formation, especially at the molecular level, have not been investigated in depth. Only a small number of reports on the "cut here line" in insects have been published,[1,10–12] and none have shown the molecular mechanisms.

The fruit fly *Drosophila melanogaster* is a holometabolous insect and develops from a larva to an adult through the pupal stage of about 4 days. Unlike other insects, the cuticle of the final instar larva (third instar larva) is not shed but stays on the surface and becomes the puparium, which covers the developing pupa. In the larval cuticle of the fly, the exocuticle is absent and the procuticle consists only of the endocuticle.[12] Shortly after puparium formation (APF), apolysis, the separation of the epidermal cells from the cuticle, occurs. Subsequently, the inner part of the procuticle is digested, and the outer part is sclerotized and tanned.[10,13] During eclosion, the emerging adult fly pushes up the operculum (anterior-dorsal region of the puparium) by inflating the ptilinum on the head to open the puparium (Figures 1A–1A‴ and Video S1). The edge of the operculum, which is called the operculum ridge (OR), corresponds to the "cut here line" on the puparium.

Here, we demonstrate that the proper formation of OR involves Notch signaling activity in the epidermal cells just beneath the future OR region (hereafter referred to as OR-forming cells) during the third instar.

[1]Department of Integrated Biosciences, Graduate School of Frontier Sciences, the University of Tokyo, Biosciences Building 501, 5-1-5 Kashiwanoha, Kashiwa-shi, Chiba 277-8562, Japan

[2]Present address: Laboratory for Extracellular Morphogenesis, Graduate School of Science, Chiba University, 1–33 Yayoi-cho, Inage-ku, Chiba-shi, Chiba 263–8522, Japan

[3]Lead contact

*Correspondence: tkojima@k.u-tokyo.ac.jp

https://doi.org/10.1016/j.isci.2023.107279

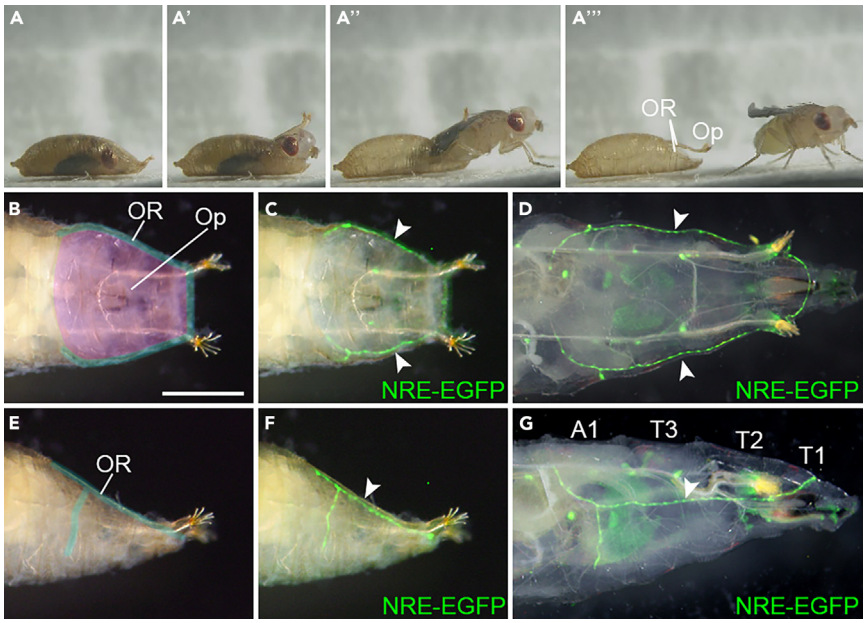

Figure 1. Eclosion process and NRE-EGFP expression in OR-forming cells

(A–A‴) Eclosion process captured from Video S1.

(B–G) Anterior part of the puparium just after its formation (B, C, E, and F) and of the late third-instar larva (D and G). (B–D) are dorsal views and (E–G) are lateral views. Anterior is to the right in (B–G) and dorsal is to the top in (E–G). The operculum (Op) and operculum ridge (OR) are colored in magenta and light green, respectively, in (B and E). NRE-EGFP signals are shown in green in (C, D, F, and G). T1–A1, 1st thoracic segment to 1st abdominal segment, respectively. Scale bar in (B), 500 μm for (B–G).

See also Video S1.

When Notch signaling was suppressed, the OR did not seem to be broken, even though flies tried hard to open the operculum, resulting in the failure of eclosion. The chitin distribution and localization of several cuticular proteins in the future OR region on the third instar larval cuticle differed from those in surrounding regions, indicating that the specialized structure is already formed during the third instar. The formation of the specialized structure was regulated by Notch signaling. In addition, we find that the enzymatic activity of glucose dehydrogenase (Gld), whose mutants show defects in OR cleavage,[14] along the OR was also regulated by Notch signaling and that Gld activity is required for the maturation of the OR during the pupal stage. Furthermore, the shape of OR-forming cells was also regulated by Notch signaling. These results suggest that Notch signaling generates the OR by regulating the formation of the specialized structure on the cuticle during the third instar and activating Gld. This is the first report on the molecular basis of the structure and formation of the "cut here line" on the cuticle.

RESULTS

Notch signaling is activated in OR-forming cells by Serrate during the late third instar

The OR begins at the anterior margin of the puparium, which is in the first thoracic segment (T1) and between the anterior spiracles, runs laterally through the second and third thoracic segments (T2 and T3, respectively), and ends within the first abdominal segment (A1). The OR runs just below the anterior spiracles in T2 and is branched dorsally and ventrally in A1 (Figures 1B and 1E). In the fly with the *NRE-EGFP* construct, which expresses EGFP in response to Notch signaling,[15] we observed strong EGFP signals in epidermal cells just beneath the OR immediately APF when epidermal cells are still attached to the cuticle (Figures 1C and 1F). Strong EGFP signals were already observed during the third instar (Figures 1D and 1G), consistent with the formation of the puparium from the cuticle of the third instar larva. When *Notch* was knocked down by RNAi in epidermal cells in the posterior compartment of each segment by crossing *engrailed* (*en*)-GAL4 with UAS-*Notch*RNAi line (*en*>*Notch*RNAi), NRE-EGFP signals disappeared in the posterior compartment (Figures 2C and 2C′), confirming that EGFP expression in OR-forming cells indeed reflects the activation of Notch signaling in these cells. To determine which ligand, Delta (Dl) or Serrate (Ser), activates Notch in OR-forming cells, either *Dl* or *Ser* was knocked down in the posterior compartment

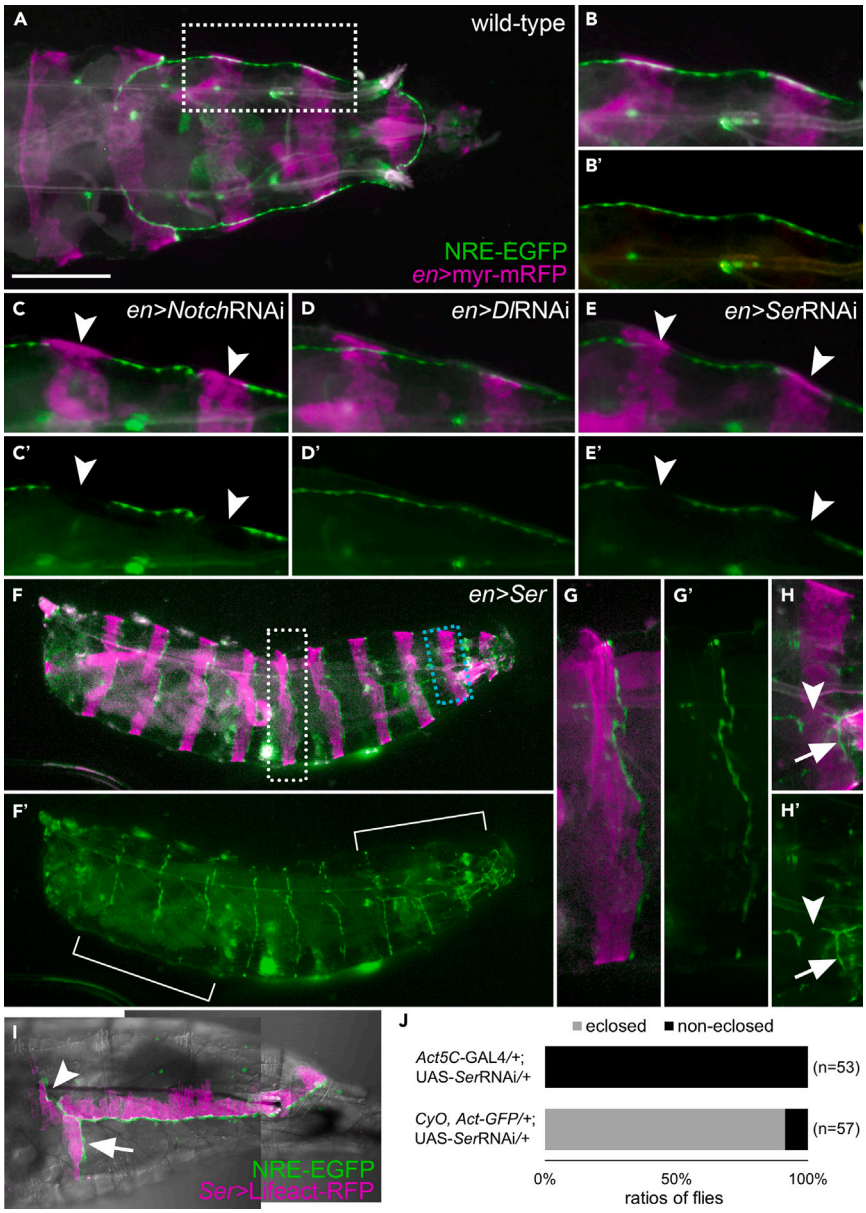

Figure 2. Activation of Notch signaling in OR-forming cells by Ser

(A–H′) NRE-EGFP signals (green) and *en*-GAL4 expression (magenta) in late third-instar larvae of *en*-GAL4 only (A–B′), *en>Notch*RNAi (C and C′), *en>Dl*RNAi (D, D′), *en>Ser*RNAi (E, E′), and *en>Ser* (F–H′).

(B and B′) are magnified views of the dotted rectangle in (A).

(C–E′) are regions corresponding to the dotted rectangle in (A). The white and light blue rectangles in (F) are magnified in (G, G′) and (H, H′), respectively. NRE-EGFP signals disappear in cases of *Notch*RNAi (C, C′, arrowheads) and *Ser*RNAi (E and E′, arrowheads) but not *Dl*RNAi (D and D′). NRE-EGFP is ectopically induced along the ectopic *Ser*-expressing region (F–H′). In T1–T3, endogenous NRE-EGFP is repressed in the ectopic *Ser*-expressing region (arrowhead in H′), while ectopic NRE-EGFP is induced along the ectopic *Ser*-expressing region (arrow in H′). NRE-EGFP is not induced by ectopic *Ser* expression in the anterior-dorsal and posterior-ventral regions (indicated by right and left brackets in F′, respectively).

(I) *Ser* expression pattern revealed by *Ser*>UAS-*Lifeact-RFP*. *Ser* (magenta) is expressed dorsally along NRE-EGFP signals in T1–T3 and the anterior half of A1, and posterior to the dorsal branch and ventral branch of NRE-EGFP signals in the posterior half of A1 (arrowheads and arrow in I, respectively).

(J) Eclosion rate of control (CyO, Act-GFP/+; UAS-*Ser*RNAi) and *Ser*RNAi (*Act5C*-GAL4/+; UAS-*Ser*RNAi) flies. Note the failure to eclose in *Ser*RNAi flies. Anterior is to the right in (A–I) and dorsal to the top in (F–I). Scale bar in (A), 500 μm for (A), 300 μm for (B–E′ and G–H′), 1000 μm for (F and F′), and 450 μm for (I).

See also Figures S1–S3 and Video S2.

by RNAi by crossing *en*-GAL4 with UAS-*Dl*RNAi or UAS-*Ser*RNAi lines (*en>Dl*RNAi or *en>Ser*RNAi, respectively). In the case of *Dl* knockdown, no obvious change in NRE-EGFP signals was observed (Figures 2D and 2D′). By contrast, NRE-EGFP signals disappeared in response to *Ser* knockdown, as in the case of *Notch* knockdown (Figures 2E and 2E′). These results were confirmed by using different RNAi lines for each gene (Figure S1). In addition, ectopic expression of *Ser* in the posterior compartment using *en*-GAL4 (*en>Ser*) induced ectopic NRE-EGFP signals along anterior-posterior compartment boundaries (Figures 2F–2H′). These results indicate that Notch signaling is activated in OR-forming cells by Ser but not Dl. Interestingly, endogenous NRE-EGFP signals disappeared in OR-forming cells in the posterior compartment of T1–T3 in the *en>Ser* fly (Figures 2H and 2H′). This may be a result of *cis*-inhibition, in which Notch activation is inhibited by the interaction with ligands on the same cell surface.[16–18] In addition, we did not detect ectopic NRE-EGFP signals in the dorsal region of T1–T3 or the ventral region of A7–A9 (Figure 2F′, brackets). Thus, Notch signaling activity may be repressed in these regions.

Consistent with Ser but not Dl acting as a ligand for Notch activation in OR-forming cells, examination of *Ser* or *Dl* expression pattern using *Ser*-GAL4 or *Dl*-GAL4 flies (see STAR Methods), respectively, showed that *Ser* was expressed in two to three rows of cells along but not overlapping with NRE-EGFP signals in OR-forming cells (Figure 2I), while *Dl* was not expressed in such a pattern (Figure S2A). Interestingly, *Ser* expression was observed just dorsal to OR-forming cells in T1–T3 and the anterior half of A1, while it was detected just posterior to the dorsal and ventral branches of OR in the posterior half of A1 (Figure 2I, arrowhead and arrow, respectively).

Notch signaling is required for the proper breakage of the OR

To evaluate the relationship between OR and Notch signaling in OR-forming cells, *Ser*RNAi was induced in all cells using *Act5C*-GAL4 to repress Notch signaling. As shown in Figure 2J, *Ser* knockdown flies failed to eclose. Although pharate adults attempted to eclose by inflating the ptilinum on their heads and actively pushing up the operculum, they appeared to be unable to break the OR (Video S2) and finally died with showing the "anteriorly jammed" phenotype, in which their heads jammed into the anterior puparium (Figures S2B and S2C). When the anterior portion of the puparium was artificially removed to partially open the operculum, the *Ser* knockdown flies were able to come out until they were trapped by the partially opened puparium (Figure S2D). In *en>Ser*RNAi flies, only a small portion of the puparium was opened, probably reflecting the striped expression of *en*-GAL4, and the majority of flies showed the "anteriorly jammed" phenotype (Figure S2E). A small number of flies tried to force their way out of the puparium from the small opening but were trapped on the way and could not eclose completely (Figure S2F). These observations indicate the requirement for Notch signaling in proper OR formation. Furthermore, over 60% of flies (213 flies in a total of 317 flies) showed the "anteriorly jammed" phenotype and failed to eclose (Figures S3A and S3B), when *Notch*RNAi was induced by GMR10G01-GAL4, in which *GAL4* is expressed specifically in OR-forming cells as described in the following (see Figure 3). The incomplete penetration of the phenotype may be due to the fact that *GAL4* expression in GMR10G01-GAL4 itself is dependent on Notch signaling (see Figure 3). This result suggests that the Notch signaling activity in OR-forming cells is important.

The characteristic structure is already made on the cuticle at the future OR region by Notch signaling during the third instar

To understand why the inhibition of Notch signaling makes the OR uncleavable, we investigated the structural aspects of the cuticle at the future OR region of late third-instar larvae. We detected chitin in the larval cuticle by staining using Calcofluor White. At low resolutions, almost no chitin staining was detected at the future OR region just above OR-forming cells expressing NRE-EGFP, unlike the surrounding cuticle (Figures 4B–4B″). However, many fine, filamentous signals were detected at the future OR region by super-resolution microscopy (Figure 4D). Furthermore, electron microscopic observations revealed that the regular pattern of the procuticle was interrupted at the future OR region, and instead, some amorphous structure was present there (Figures S4A and S4A′). These observations suggest that a specialized structure is already formed at the future OR region on the late third-instar larval cuticle before its change to the puparium (Figure 4C). In *en>Notch*RNAi and *en>Ser*RNAi, the chitin staining pattern specific to the future OR region was lost (Figures 4E–4F″). By contrast, in *en>Ser* flies, the region of weak chitin staining appeared along cells expressing *Ser* ectopically (Figures 4G–4G″). Furthermore, in GMR10G01>*Notch*RNAi flies, the chitin staining pattern at the future OR region was partially disrupted (Figure S3C and S3C′). These results

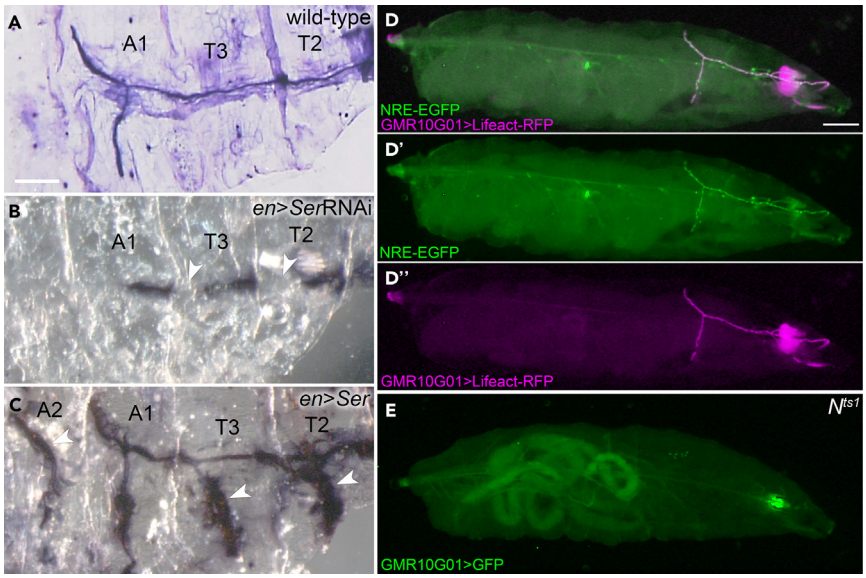

Figure 3. Gld activity and its dependency on Notch signaling

(A–C) Gld activity staining in mid-third instar larvae of wild-type (A), *en>Ser*RNAi (B), and *en>Ser* (C) flies. The signal is abolished in *Ser*RNAi domains (arrowheads in B) and is ectopically induced along with ectopic *Ser* expression (arrowheads in C).

(D–D″) Expression patterns of NRE-EGFP and GMR-GAL4-driven Lifeact-RFP. Note that NRE-EGFP and Lifeact-RFP signals are completely overlapped in the OR-forming cells.

(E) GMR10G01-driven GFP expression pattern in the temperature-sensitive *Notch* mutant at non-permissive temperature (29°C). Note the complete disappearance of GFP signal in OR-forming cells. Anterior is to the right and dorsal to the top in all figures. Scale bar in (A), 300 μm for (A-C), and Scale bar in (D), 500 μm for (D–E).

See also Figure S6.

indicate that the formation of the specialized structure at the future OR region, as revealed by the specific chitin distribution, is dependent on Notch signaling in OR-forming cells.

We next examined the localization of three cuticular proteins, Obstructor-E-a (Obst-E-a), Cuticular protein 11A (Cpr11A), and Tubby (Tb), using transgenic flies with an insertion of a genomic fragment in which each gene is tagged with GFP or EGFP.[5,7,8] In the *Drosophila* larval cuticle, Obst-E-a is localized at the procuticle, Tb at the epicuticle, and Cpr11A around the interface between the procuticle and epicuticle.[5,7,8] As shown in Figures 5C and 5C′, we detected stronger Obst-E-a-GFP signals at the future OR region than in the surrounding region. In contrast to the chitin staining signal, no fine structure was observed even when examined by the super-resolution microscope (Figure S5). Cpr11A-EGFP signals were excluded from the future OR region (Figures 5E and 5E′). Furthermore, strong signals were also observed at the future OR region in the case of Tb-GFP (Figures 5G and 5G′). These observations suggest that in addition to the specialized structure revealed by chitin staining, the localization of cuticular proteins is already changed at the future OR region in the late third instar before puparium formation (Figure 5B). When Notch signaling was inhibited by *Ser*RNAi using *en*-GAL4, specific localization patterns of Obst-E-a, Cpr11A, and Tb disappeared (Figures 5D, 5F, and 5H), indicating that the activation of Notch signaling in OR-forming cells regulates the localization of these cuticular proteins at the future OR region during the third instar.

Expression of Gld is positively regulated by Notch signaling in OR-forming cells

By activity staining, Gld activity has been reported to be observed specifically in OR-forming cells during the third instar[19] (Figure 3A), and we found this activity becomes detectable at the late second-instar stage (Figures S6A and S6B). Gld activity was lost in OR-forming cells in which Notch signaling is inactivated in *en>Ser*RNAi flies (Figure 3B), indicating the positive regulation of Gld activity by Notch signaling. Consistent with this observation, ectopic Gld activity was induced along cells ectopically expressing *Ser* in *en>Ser* flies (Figure 3C).

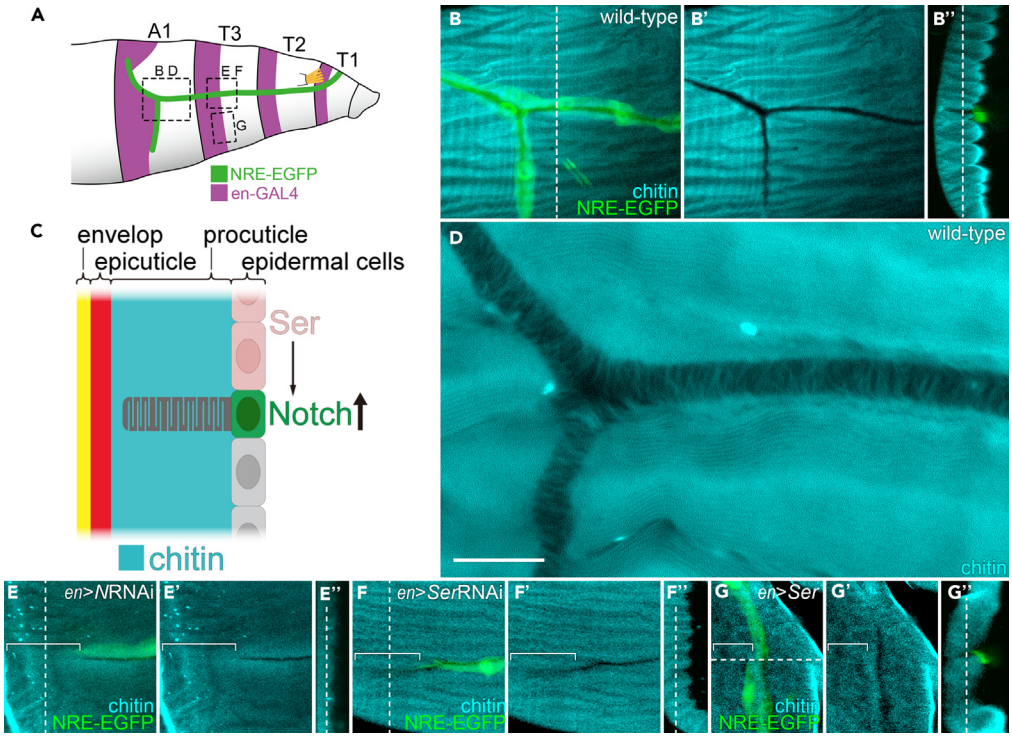

Figure 4. Specialized chitin staining at the late third instar and its dependency on Notch signaling

(A) Schematic drawing showing NRE-EGFP and *en*-GAL4 expression patterns. Dotted rectangles labeled BD, EF, and G correspond to regions shown in (B–B″, D), (E–F″), and (G–G″), respectively.

(B–B″, E–G″) chitin staining patterns in wild-type (B–B″, D), *en>Notch*RNAi (E–E″), *en>Ser*RNAi (F–F″), and *en>Ser* (G–G″), respectively. (B″, E″, F″, and G″) show cross-sectional views at broken lines in (B, E, F, and G), respectively. (B, B′, E, E′, F, F′, G, G′) are the plane of focus indicated by broken lines in (B″, E″, F″, and G″), respectively. In (B, E, F, and G), chitin staining signals and NRE-EGFP signals on different planes of focus are merged. Brackets in (E, E′, F, F′, G, G′) indicate *en*RNAi (E, E′), *Ser*RNAi (F, F′) and ectopic Ser expression (G, G′) domains.

(C) A schematic summary showing the chitin staining pattern at the late third instar stage. At the future OR region, the chitin staining signal is greatly reduced at low resolution (B–B″), while fine, filamentous signals are detected at high resolution (D). The regions with highly reduced chitin signals disappear in *Notch*RNAi (E–E″) and *Ser*RNAi (F–F″) domains but are ectopically induced along the ectopic *Ser* expression domain. Anterior is to the right and dorsal to the top in (A, B, B′, D, E, E′, F, F′, G, G′). Outside of the body is to the left in (B″, C, E″, F″, G″). Scale bar in (D), 200 μm for (B–B″, E–G″) and 6.5 μm for (D).

See also Figures S3 and S4.

Among several GAL4 lines, in which genomic fragments from the *Gld* locus drive *GAL4* expression,[20] we found that GMR10G01-GAL4 expresses *GAL4* in OR-forming cells and anterior spiracles (Figures 3D–3D″ and S6C). In the temperature-sensitive mutant of *Notch*, which was shifted to the non-permissive temperature at 29°C from the early second instar, only the expression in anterior spiracles could be observed and the expression in OR-forming cells disappeared (Figure 3E). Thus, Notch signaling appears to regulate the transcription of *Gld*. By contrast, no change in NRE-EGFP signal intensity was detected in *Gld* mutants (Figure 6B). Together with the results of activity staining, these observations indicate that Gld activity is positively regulated downstream of Notch signaling in OR-forming cells at least through the transcriptional regulation.

Gld is required for OR maturation

It has been reported that *Gld* mutants appear to be unable to eclose due to the failure in opening the OR since the manual excision of the anterior portion of the puparium rescued the lethality of *Gld* mutants.[14] Gld activity begins to be detected strongly in all epidermal cells by the late third instar;[19] however, it remained unknown whether the failure of eclosion occurs due to Gld activity in OR-forming cells, in all epidermal cells, or both. To evaluate these possibilities, *Gld* was knocked down by RNAi using

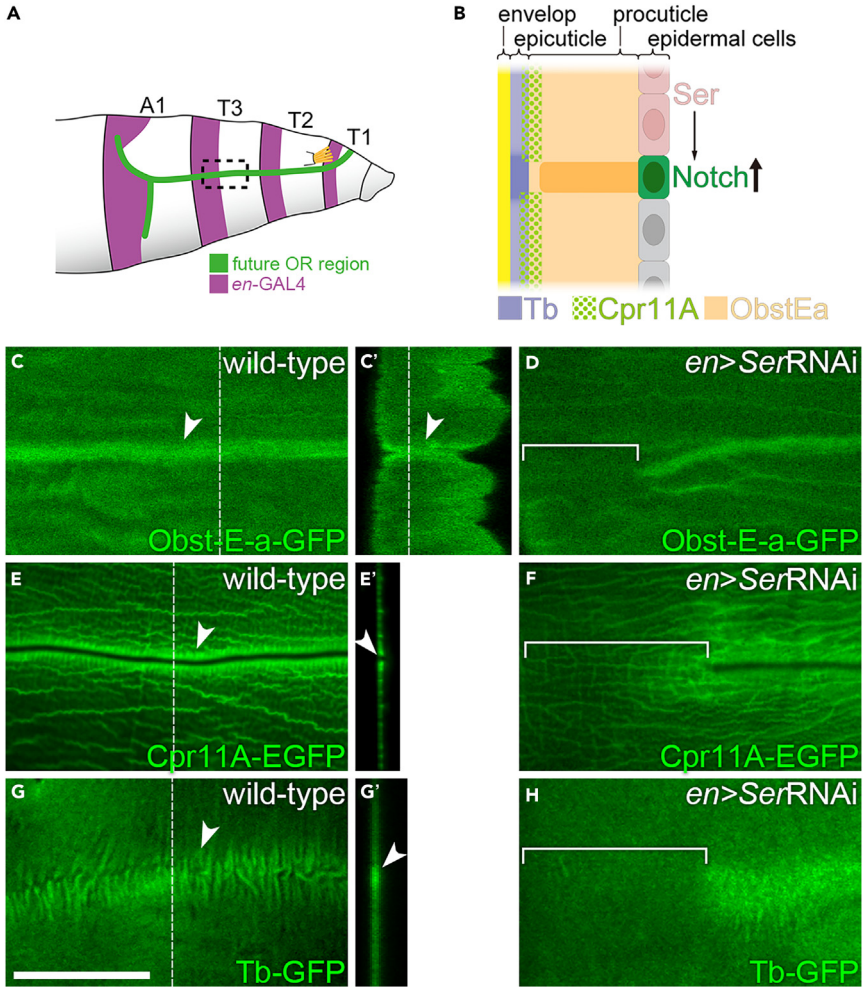

Figure 5. Localization patterns of cuticular proteins at the late third instar and their dependency on Notch signaling

(A) Schematic drawing showing the future OR region and *en*-GAL4 expression patterns at the late third instar. The dotted rectangle corresponds to regions shown in (C–H).

(B) Schematic summary of cuticular protein localization.

(C–H) Localization patterns of Obst-E-a-GFP (C-D), Cpr11A-EGFP (E-F), and Tb-GFP (G-H) in wild-type (C, C′, E, E′, G, G′) and *en>Ser*RNAi (D, F, H) flies. (C′, E′, G′) show cross-sectional views at broken lines in (C, E, G), respectively. The plane of focus in (C) is indicated by the broken line in (C′). Arrowheads, the future OR regions. Brackets in (D, F, H), *en>Ser*RNAi domains. In wild-type, Obst-E-a-GFP and Tb accumulate at the OR region, while Cpr11A-GFP is excluded. These specific localization patterns disappear in *en>Ser*RNAi domains. Anterior is to the right and dorsal to the top in (A, C, D, E, F, G, H). Outside of the body is to the left in (B, C′, E′, G′). Scale bar in (G), 50 μm for (C–H).

See also Figure S5.

GMR10G01-GAL4 and two different *Gld*RNAi lines. In both cases, GMR10G01>*Gld*RNAi flies failed to eclose and showed the "anteriorly jammed" phenotype (Figures S6D–S6E′), indicating that Gld activity in OR-forming cells is indispensable for normal OR formation.

To determine the function of Gld in normal OR formation, we examined the distribution of chitin, Tb, Cpr11A, and Obst-E-a in *Gld* mutants at the late third instar. Surprisingly, we did not observe clear differences between *Gld* mutants and wild-type flies (Figures 6B–6E). Furthermore, even in electron microscopic observation, we could not detect obvious differences between wild-type and *Gld* mutants (Figures S4A–S4B′). These results indicate that Gld may contribute to the process other than the regulation of chitin, Tb, Cpr11A, and Obst-E-a at the future OR region in the late third instar.

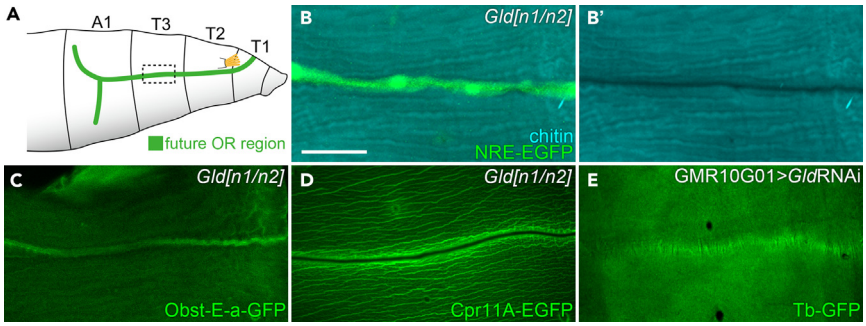

Figure 6. Dispensability of Gld for the specific chitin staining signal and Obst-E-a, Cpr11A, and Tb localization at the future OR region in the late third instar larval cuticle

(A) Schematic drawing showing the future OR region at the late third instar. The dotted rectangle corresponds to regions shown in (B–E).

(B–E) Chitin staining signal (B and B′) and localization pattern of Obst-E-a-GFP (C), Cpr11A-EGFP (D), and Tb-GFP (E) in *Gld* mutants (B–D) or *Gld*RNAi flies (E). Note the lack of obvious defects. Anterior is to the right and dorsal to the top in all figures. Scale bar in (B), 50 μm for (B–E).

See also Figure S4.

To elucidate defects in *Gld* mutants, we further examined abnormalities in OR formation in the pupal stage in *Gld* mutants. Around 5 h APF, apolysis between epidermal cells and the puparium occurs in the anterior portion.[21,22] Then, around 7.5 h APF, the inner part of the puparium splits off from the outer part and is digested.[13] After this stage, the OR becomes easily cleavable, and thus dissection and chitin staining while maintaining an intact OR become difficult. To avoid this issue, we examined the state of chitin without dissection using UAS-*ChtVis-Tomato* driven by *e22c*-GAL4, in which *GAL4* is expressed in all epidermal cells. ChtVis-Tomato is a fluorescent protein fused with the chitin-binding domain and is expected to show the chitin distribution.[23] However, there was a significant difference between the ChtVis-Tomato and chitin staining signals, for unknown reasons. At the late third instar, although both signals were ubiquitously detected in the procuticle outside the future OR region, the ChtVis-Tomato signal at the future OR region was stronger than that in the adjacent region, unlike the chitin staining signal (Figures 7C and 7C′, compare with Figures 4B′ and 4B″). The distribution of the ChtVis-Tomato signal resembled that of the Obst-E-a-GFP signal (compare Figures 7C and 7C′ with Figures 5C and 5C′). In wild-type flies, the ChtVis-Tomato pattern at 4 h APF remained similar to that at the late third instar (Figures 7D and 7D′). At about 72 h APF, however, the strong ChtVis-Tomato signal disappeared, and a wedge-shaped gap was formed at the OR region (Figures 7E and 7E′). These observations indicate that part of the cuticle including the region with the strong ChtVis-Tomato signal is lost during the maturation of the OR in wild-type flies. In *Gld* mutants, the ChtVis-Tomato signal at about 72 h APF still resembled that at 4 h APF, unlike in wild-type flies (Figures 7F and 7F′). Thus, Gld appears to be required for the maturation of the OR during the pupal stage.

Notch signaling is involved in the specific shape of OR-forming cells

In the late third instar, the shape of OR-forming cells differs from that of neighboring epidermal cells, as revealed by the localization of Neuroglian-GFP (Nrg-GFP).[24] They are narrow and elongated, forming a thin line prefiguring the OR (Figures 8A–8A″ and S7). When Notch signaling was inactivated by *Notch*RNAi in all epidermal cells using *Act5C*-GAL4, the narrow, elongated cells disappeared (Figures 8B and 8B′). Similarly, when *Notch*RNAi was induced only in the posterior half of each segment using *en*-GAL4, the line of the narrow, elongated cells was disrupted in *en*-GAL4-expressing region (Figures 8C –8C"). These results indicate that the shape of OR-forming cells is also regulated by Notch signaling.

DISCUSSION

Control of OR formation by Notch signaling

Notch signaling regulates the formation of the specialized structure at the late third instar, as revealed by patterns of chitin staining and cuticular protein localization (see Figures 4 and 5). Since epidermal cells are separated from the cuticle after apolysis, they are not expected to affect the cuticle during the pupal stage. Therefore, it is quite reasonable for the specialized structure, which may become the OR during

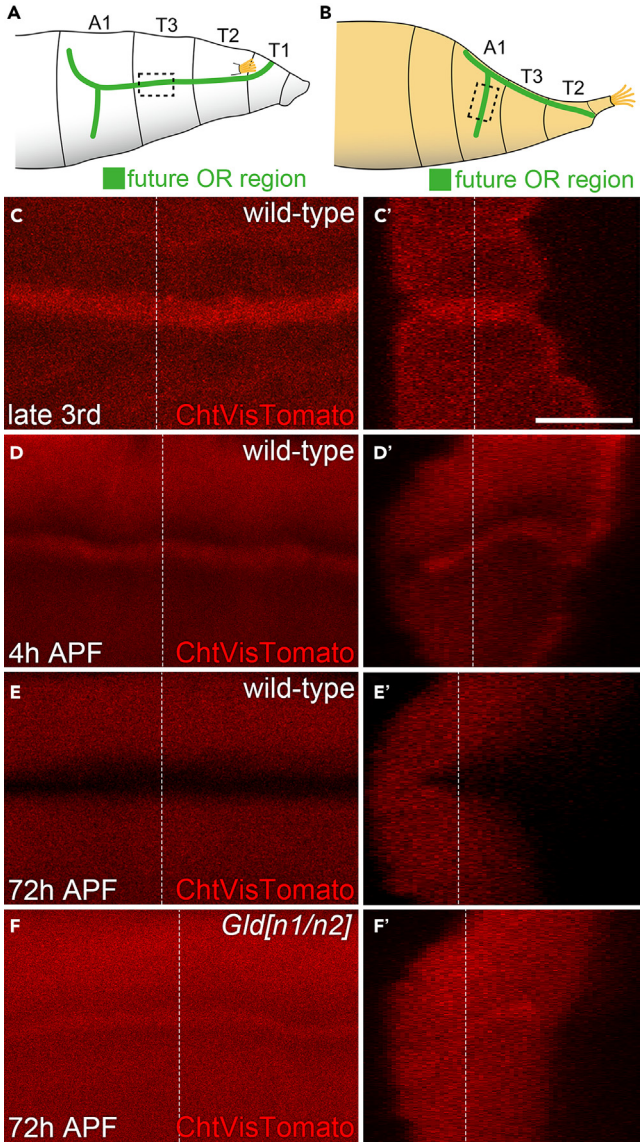

Figure 7. Requirement of Gld for OR maturation

(A and B) Schematic drawing of the future OR region at the late third instar (A) and pupal stage (B). Dotted rectangles in (A) and (B) correspond to regions shown in (C and C′) and (D–F′), respectively. (C–F′) ChtVis-Tomato signals at the late third-instar stage (C, C′), 4 h (D, D′), and 72 h (E–F′) APF in the wild-type (C–E′) and *Gld* mutant (F, F′). (C′, D′, E′, and F′) show cross-sectional views at the broken lines in (C, D, E, and F), respectively. The planes of focus in (C, D, E, and F) are indicated by broken lines in (C′, D′, E′, and F′), respectively. Strong ChtVis-Tomato signal is observed at the OR region at the late third instar stage and 4 h APF, and disappears by 72 h APF in wild-type flies, whereas signals are still observed at 72 h APF in the *Gld* mutant. Dorsal is to the top in (A–C′) and to the right in (D, E, F). Anterior is to the right in (A–C) and to the bottom in (D–F′). Outside of the body is to the left in (C′, D′, E′, F′). Scale bar in (C′), 15 μm for (C–F′).

the pupal stage, to be formed, prior to puparium formation. In addition, Notch signaling appears to regulate the maturation of the OR during the pupal stage via the regulation of Gld activity during the third instar (see Figures 3 and 7). The shape of OR-forming cells was also under the control of Notch signaling (see Figure 8). Thus, Notch signaling appears to control the whole process of OR formation. However, the shape of the outer surface of the puparium at the OR region did not depend on Notch signaling. The puparium surface is sharply bent along the OR, protruding into a mountain-like shape (see Figures 1B, 1C, 1E, 1F,7D′, and 7E′), and there seemed to be no obvious shape changes when Notch signaling was suppressed (see Figures S1B and S1C). The operculum is flat compared with the adjacent

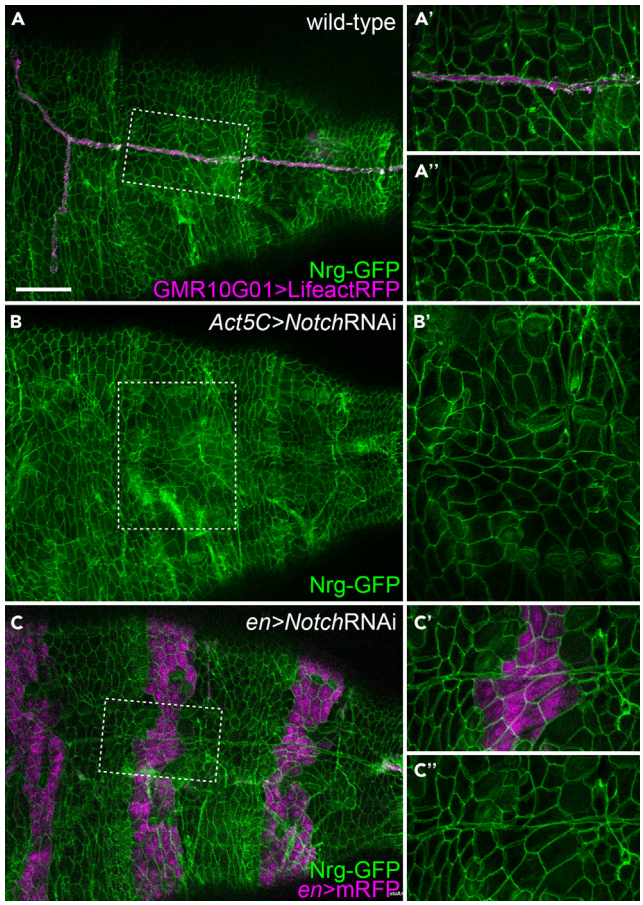

Figure 8. Regulation of the shape of OR-forming cells by Notch signaling

(A–C″) Shape of epidermal cells revealed by Nrg-GFP at the late third instar in wild-type (A–A″), *Act5C* > *Notch*RNAi (B and B′), and *en*>*Notch*RNAi (C–C″) flies. OR-forming cells in wild-type are labeled by Lifeact-RFP expression driven by GMR10G01-GAL4 (A and A′). Regions surrounded by the broken line in (A–C) are magnified in (A′, A″), (B′), and (C′, C″), respectively. Note the narrow, elongated shape of OR-forming cells in wild-type (A–A″). Cells with this characteristic shape disappear in *Act5C* > *Notch*RNAi (B and B′). When *Notch* is knocked down only in the posterior compartment cells (labeled by mRFP expression), the line of narrow, elongated cells is disrupted there (C–C″). Anterior is to the right and dorsal to the top in all figures. Scale bar in (A), 200 μm for (A, B, C) and 100 μm for (A′, A″, B′, C′, C″).
See also Figure S7 and Table S2.

region, and this flatness might cause a sharp bend at the OR region. If this is true, a mechanism independent of Notch signaling might determine differences in character between the operculum and other regions of the puparium and form the protruded shape of the OR region. Nonetheless, it is quite reasonable to consider that Notch signaling regulates all processes involved in OR formation other than the formation of the outer shape.

Specialized cuticle structure of the future OR region before puparium formation

Hadley[1] and Chapman[12] reported that at the future "cut here line" of larval hemimetabolous insects, the exocuticle is absent and the procuticle consists of only the endocuticle. Subsequent degradation of the endocuticle at the molting stage results in a mechanically weak region composed only of the envelope and epicuticle, creating the "cut here line." Moreover, it has been reported that in the blow fly *Calliphora erythrocephala*, sclerotization of the outer part of the procuticle does not occur at the future OR region during puparium formation, and the mature OR is formed by the removal of this region with the inner non-sclerotized procuticle.[10] In these reports, the cuticle structure of the future "cut here line" is described as a simple expansion of the endocuticle, which is not different from the surrounding endocuticle, at the expense of the exocuticle. Furthermore, no

specific structure is mentioned for the envelope and epicuticle. In our observations, however, a specialized structure was detected by chitin staining and patterns of cuticular protein localization (see Figures 4 and 5) at the future OR region during the late third instar. The specific localization patterns of cuticular proteins were also observed in the epicuticle (see Figure 5). Therefore, at least in the epicuticle and procuticle, the structure formed at the future "cut here line" may be more complex than previously thought.

Tb and Cpr11A have been suggested to interact with each other and confer the cuticle resistance against tensile strength along the body circumference.[7,8] The absence of Cpr11A from the future OR region may make it weaker, while an increase in Tb may strengthen the epicuticle. This balance might prevent the cuticle from breaking off accidentally during the third instar.

The localization of Obst-E-a is more intense at the future OR region than in the adjacent region (see Figure 5). A similar increase in signal is also observed in the case of ChtVis-Tomato (see Figure 7). Since both proteins can bind chitin through their chitin-binding domain,[5,23] strong signals could indicate substantial chitin accumulation at the future OR region. The chitin distribution determined by Calcofluor White showed that chitin is rather less abundant and forms a fine, filamentous structure at the future OR region. Calcofluor White is a small molecule, and both ChtVis-Tomato and Obst-E-a have larger molecular sizes. The procuticle outside the OR may be tightly packed with chitin fibers and cuticular proteins, unlike the future OR region, and therefore proteins might be relatively difficult to penetrate the non-OR procuticle and might accumulate in the future OR region. Since we used homozygotes of *Obst-E-a-GFP* for the examination of Obst-E-a distribution in wild type, these flies have four copies of *Obst-E-a* gene (two copies each of *Obst-E-a* with or without *GFP*). Thus, the amount of Obst-E-a protein may be higher in these flies than in wild-type flies. Similarly, *ChtVis-Tomato* was expressed using UAS/GAL4 system, and thus, the expression level may be very high. Therefore, there is a possibility that these higher amounts of proteins might mask the actual chitin distribution pattern. This idea is not mutually exclusive with the above idea. In any case, we think that the amount of chitin may be lower at the future OR region than in surrounding regions. The disruption of the regular patterns of the procuticle at the future OR region, which was observed by electron microscopy (see Figure S4), seems consistent with this.

Involvement of Gld in OR formation

Previous work has shown that Gld activity is observed specifically in OR-forming cells.[19] Our results indicate that Gld activity in OR-forming cells is regulated by Notch signaling at least through transcriptional regulation (see Figure 3). Consistent with this, one Su(H)-binding motif is found in the genomic fragment used in GMR10G01-GAL4 (Figure S6C). Consensus binding motifs can be found in many other regions also, however, further analysis is required to conclude the regulation of *Gld* transcription through the Su(H)-binding motif in the GMR10G01 fragment.

Although Gld activity has been reported to be observed in all epidermal cells at the late third instar,[19] the requirement for *Gld* in OR-forming cells (see Figure S6) is reasonable, since the specialized structure of the future OR region is already formed by the late third instar, and thus may be formed during the process of the third-instar larval cuticle formation. In light of this, the fact that Gld activity can be detectable at the late second instar seems also reasonable since the production of the third-instar larval cuticle is started just before the molt to the third instar larva. Gld catalyzes the conversion of glucose to gluconolactone with the reduction of the tightly bound co-factor flavin adenine dinucleotide (FAD) to $FADH_2$. It has been proposed that Gld could be involved in cuticle modification or degradation by generating free radicals via $FADH_2$ production.[25] This activity might eventually lead to the removal of a part of the cuticle containing strong ChtVis-Tomato signals from the OR region.

While OR maturation during the pupal stage was disturbed in *Gld* mutants, Gld appeared to be dispensable for the chitin distribution and the localization of Tb, Cpr11A, and Obst-E-a at the late third instar (see Figures 6 and 7). Furthermore, no apparent difference between wild-type and *Gld* mutants could be observed in the electron microscopic observation of the future OR region (see Figure S4). These results do not necessarily mean that Gld does not function during the third-instar stage. It is possible that Gld influences a different structure than that we observed here and/or properties of some factors that are not reflected in the structure of the future OR region at the late third instar and that this unknown structure and/or properties are important for OR maturation during the pupal stage. Alternatively, considering that Gld is secreted,[25] Gld produced by OR-forming cells during the third instar might be incorporated

into the future OR region during its formation and remains there to exert functions during the pupal stage. These two explanations are not mutually exclusive. Further analysis of Gld would lead to the understanding of the mechanism underlying the change from the future OR region to the mature OR.

Determination of the OR position

Notch signaling is activated in OR-forming cells by Ser (see Figure 2). Thus, the OR position is determined by the spatial and temporal pattern of *Ser* expression. OR-forming cells run along the anteroposterior axis in T1–T3 and anterior A1, and their position has been suggested to coincide with the dorsal/ventral compartment boundary.[26] Thus, a simple possibility is that *Ser* is expressed in all cells dorsal or ventral to OR-forming cells. In this case, the *Ser* expression pattern could be simply determined by a signal emanating from the dorsal or ventral midline, and the activation of Notch signaling could be easily restricted to a single line of cells at the interface between *Ser*-positive and *Ser*-negative cells. Our observations, however, do not support this explanation. In T1–T3 and anterior A1, *Ser* is expressed in cells immediately dorsal to OR-forming cells but is restricted to a row of two to three cells wide (Figure 2I). This *Ser* expression pattern could lead to the activation of Notch signaling in two lines of cells, both dorsal and ventral to the *Ser*-expressing region. In the experiment of ectopic *Ser* expression, we found that Notch signaling is not activated in the region dorsal to OR-forming cells (Figures 2H and 2H′). Therefore, the activation of Notch signaling may be inhibited in the dorsal region and restricted to the ventral side of the *Ser*-expressing cells. The expression of *Ser* in a row of cells indicates that the regulation of *Ser* expression is not simple. A combination of repression and activation by factors determining the properties of the dorsoventral axis might be important.

In the posterior half of A1, OR is branched dorsally and ventrally. In this region, *Ser* is expressed posteriorly along these branched OR-forming cells (Figure 2H, arrowhead and arrow, respectively). Thus, *Ser* appears to have at least two independent enhancers, one regulating the expression in T1–T3 and anterior A1, and another regulating the expression in the posterior half of A1. Interestingly, it has been reported that *Hox* genes control the branched shape of the OR in the posterior half of A1.[27] Thus, the latter enhancer may be regulated by *Hox* genes. The identification and analysis of regulatory elements for OR-related *Ser* expression are important to understand how the OR position is determined.

Evolutionary perspective on the "cut here line"

In many insect species, the "cut here line" is formed at the dorsal midline of the thorax. From this point of view, the OR might be a special "cut here line" having arisen only in the lineage leading to *D. melanogaster*. Interestingly, however, Gld activity has been reported to be detected along the "cut here line" of larvae of *Manduca sexta* (Lepidoptera), although this was not described in detail.[25] This may imply that at least some of the formation mechanism is conserved between OR and the "cut here line" of other insect species, with alterations in its position via changes in *Ser* expression pattern. In addition, in *Elenchus tenuicornis*, a strepsipteran insect species forming the puparium during metamorphosis,[28] it has been reported that the exocuticle is not colored and sclerotized at the future "cut here line," unlike the adjacent cuticle. Electron microscopy showed that this region has a unique structure and is not a simple expansion of the endocuticle.[11] The formation of the unique structure at the "cut here line" resembles our findings on the OR and may imply some similarities between the "cut here lines" of *E. tenuicornis* and *D. melanogaster*. Further examinations of the "cut here line" structure, the function of Notch signaling, and *Ser* expression patterns in other insect species will help to reveal similarities and differences and provide insight into the evolution of the "cut here line" in insects. Furthermore, the position of the "cut here line" is largely specific to each subphylum of Arthropoda (i.e., Chelicerate, Myriapod, Crustacean, and Hexapod). Thus, investigations of the "cut here line" in these taxa will lead to a better understanding of the evolution not only of insects but also of arthropods in general.

Limitations of the study

The fragility of the puparium makes chitin staining using Calcofluor White difficult. Accordingly, we were not able to observe how the fine, filamentous chitin signal changes during the pupal stage and in the final OR. In addition, the mechanism by which Notch signaling controls the distribution of chitin and localization of cuticular proteins, as well as the mechanism of action of Gld, is not clear. Resolving these issues will further improve our understanding of the molecular basis of the "cut here line" on the cuticle.

STAR★METHODS

Detailed methods are provided in the online version of this paper and include the following:

- KEY RESOURCES TABLE
- RESOURCE AVAILABILITY
  - Lead contact
  - Materials availability
  - Data and code availability
- EXPERIMENTAL MODEL AND SUBJECT DETAILS
  - Fly stocks and genetics
- METHOD DETAILS
  - Chitin staining
  - Gld activity staining
  - Microscopy
  - Observation of ChitVis-Tomato signals in the pupal stage
- QUANTIFICATION AND STATISTICAL ANALYSIS

SUPPLEMENTAL INFORMATION

Supplemental information can be found online at https://doi.org/10.1016/j.isci.2023.107279.

ACKNOWLEDGMENTS

We thank the Kyoto Stock Center, the Bloomington Stock Center, the Vienna Drosophila Resource Center, and Bernard Moussian for fly stocks. This work was supported by the Japan Society for the Promotion of Science (JSPS) Research Fellowships (15J40022 and 19J40012 to R.T.), JSPS Grants-in-Aid for Scientific Research (20K06666 to R.T. and 18K06243 to T.K.), Grant-in-Aid for Scientific Research on Innovative Areas from the Ministry of Education, Culture, Sports, Science, and Technology (MEXT) (18H04758 and 20H05945 to R.T. and 21H05773 and 23H04303 to T.K.), the Naito Foundation (to R.T.), Tomizawa Jun-ichi & Keiko Fund of Molecular Biology Society of Japan for Young Scientist (to R.T.), Shiseido Female Researcher Science Grant (to R.T.), Takeda Science Foundation (2022034459 to R.T.), and Suntory Rising Stars Encouragement Program in Life Sciences (SunRiSE) (to R.T.).

AUTHOR CONTRIBUTIONS

R.T. and T.K. designed the experiments. R.T., A.H., Y.K., D.T., Z.C., and T.K. performed the experiments and analyzed the data. R.T. and T.K. wrote the manuscript.

DECLARATION OF INTERESTS

The authors declare no competing interests.

Received: January 17, 2023
Revised: May 25, 2023
Accepted: June 30, 2023
Published: July 4, 2023

REFERENCES

1. Hadley, N.F. (1986). The Arthropod cuticle. Sci. Am. *255*, 104–112.

2. Moussian, B. (2013). The Arthropod cuticle. In Arthropod Biology and Evolution, A. Minelli, ed. (Berlin, Heidelberg: Springer Berlin Heidelberg), pp. 171–196.

3. Qiao, L., Xiong, G., Wang, R.X., He, S.Z., Chen, J., Tong, X.L., Hu, H., Li, C.L., Gai, T.T., Xin, Y.Q., et al. (2014). Mutation of a cuticular protein, BmorCPR2, alters larval body shape and adaptability in silkworm, Bombyx mori. Genetics *196*, 1103–1115. https://doi.org/10.1534/genetics.113.158766.

4. Tajiri, R. (2017). Cuticle itself as a central and dynamic player in shaping cuticle. Curr. Opin. Insect Sci. *19*, 30–35. https://doi.org/10.1016/j.cois.2016.10.009.

5. Tajiri, R., Ogawa, N., Fujiwara, H., and Kojima, T. (2017). Mechanical control of whole body shape by a single cuticular protein obstructor-E in Drosophila melanogaster. PLoS Genet. *13*, e1006548. https://doi.org/10.1371/journal.pgen.1006548.

6. Xiong, G., Tong, X., Gai, T., Li, C., Qiao, L., Monteiro, A., Hu, H., Han, M., Ding, X., Wu, S., et al. (2017). Body shape and coloration of silkworm larvae are influenced by a novel cuticular protein. Genetics *207*, 1053–1066. https://doi.org/10.1534/genetics.117.300300.

7. Zuber, R., Wang, Y., Gehring, N., Bartoszewski, S., and Moussian, B. (2020). Tweedle proteins form extracellular two-dimensional structures defining body and cell shape in Drosophila melanogaster. Open Biol. *10*, 200214. https://doi.org/10.1098/rsob.200214.

8. Tajiri, R., Fujiwara, H., and Kojima, T. (2021). A corset function of exoskeletal ECM promotes

body elongation in Drosophila. Commun. Biol. *4*, 88. https://doi.org/10.1038/s42003-020-01630-9.

9. Tan, D., Hu, H., Tong, X., Han, M., Gai, T., Lou, J., Yan, Z., Xiong, G., Lu, C., and Dai, F. (2022). Mutation of a lepidopteran-specific PMP -like protein, BmLSPMP -like, induces a stick body shape in silkworm, Bombyx mori. Pest Manag. Sci. *78*, 5334–5346. https://doi.org/10.1002/ps.7156.

10. Whitten, J.M. (1957). The supposed Pre-pupa in Cyclorrhaphous Diptera. J. Cell Sci. *s3–98*, 241–249.

11. Kathirithamby, J., Luke, B.M., and Neville, A.C. (1990). The ultrastructure of the preformed ecdysial 'line of weakness'' in the puparium cap of Elenchus tenuicornis (Kirby) (Insecta: Strepsiptera). Zool. J. Linn. Soc. *98*, 229–236. https://doi.org/10.1111/j.1096-3642.1990.tb01208.x.

12. Chapman, R.F. (1998). Integument. In The Insects, R.F. Chapman, ed. (Cambridge University Press), pp. 415–440. https://doi.org/10.1017/CBO9780511818202.017.

13. Poodry, C.A., and Schneiderman, H.A. (1970). The ultrastructure of the developing leg of Drosophila melanogaster. Wilhelm Roux. Arch. Entwickl. Mech. Org. *166*, 1–44. https://doi.org/10.1007/BF00576805.

14. Cavener, D.R., and MacIntyre, R.J. (1983). Biphasic expression and function of glucose dehydrogenase in Drosophila melanogaster. Proc. Natl. Acad. Sci. USA *80*, 6286–6288. https://doi.org/10.1073/pnas.80.20.6286.

15. Saj, A., Arziman, Z., Stempfle, D., van Belle, W., Sauder, U., Horn, T., Dürrenberger, M., Paro, R., Boutros, M., and Merdes, G. (2010). A combined ex vivo and in vivo RNAi screen for notch regulators in Drosophila reveals an extensive notch interaction network. Dev. Cell *18*, 862–876. https://doi.org/10.1016/j.devcel.2010.03.013.

16. Becam, I., Fiuza, U.M., Arias, A.M., and Milán, M. (2010). A role of receptor notch in ligand cis-inhibition in Drosophila. Curr. Biol. *20*, 554–560. https://doi.org/10.1016/j.cub.2010.01.058.

17. del Álamo, D., Rouault, H., and Schweisguth, F. (2011). Mechanism and significance of cis-inhibition in notch signalling. Curr. Biol. *21*, 40–47. https://doi.org/10.1016/j.cub.2010.10.034.

18. Fleming, R.J., Hori, K., Sen, A., Filloramo, G.V., Langer, J.M., Obar, R. a, Artavanis-Tsakonas, S., and Maharaj-Best, A.C. (2013). An extracellular region of Serrate is essential for ligand-induced cis-inhibition of Notch signaling. Development *140*, 2039–2049. https://doi.org/10.1242/dev.087916.

19. Ross, J.L., Fong, P.P., and Cavener, D.R. (1994). Correlated evolution of the cis-acting regulatory elements and developmental expression of the Drosophila Gld gene in seven species from the subgroup melanogaster. Dev. Genet. *15*, 38–50. https://doi.org/10.1002/dvg.1020150106.

20. Jenett, A., Rubin, G.M., Ngo, T.T.B., Shepherd, D., Murphy, C., Dionne, H., Pfeiffer, B.D., Cavallaro, A., Hall, D., Jeter, J., et al. (2012). A GAL4-driver line resource for Drosophila neurobiology. Cell Rep. *2*, 991–1001. https://doi.org/10.1016/j.celrep.2012.09.011.

21. Fraenkel, G., and Bhaskaran, G. (1973). Pupariation and pupation in Cyclorrhaphous flies (Diptera): terminology and interpretation1. Ann. Entomol. Soc. Am. *66*, 418–422. https://doi.org/10.1093/aesa/66.2.418.

22. Bainbridge, S.P., and Bownes, M. (1981). Staging the metamorphosis of Drosophila melanogaster. J. Embryol. Exp. Morphol. *66*, 57–80.

23. Sobala, L.F., Wang, Y., and Adler, P.N. (2015). ChtVis-Tomato, a genetic reporter for *in vivo* visualization of chitin deposition in *Drosophila*. Development *142*, 3974–3981. https://doi.org/10.1242/dev.126987.

24. Morin, X., Daneman, R., Zavortink, M., and Chia, W. (2001). A protein trap strategy to detect GFP-tagged proteins expressed from their endogenous loci in Drosophila. Proc. Natl. Acad. Sci. USA *98*, 15050–15055. https://doi.org/10.1073/pnas.261408198.

25. Cox-Foster, D.L., and Stehr, J.E. (1994). Induction and localization of FAD-glucose dehydrogenase (GLD) during encapsulation of abiotic implants in Manduca sexta larvae. J. Insect Physiol. *40*, 235–249. https://doi.org/10.1016/0022-1910(94)90047-7.

26. Segal, D., and Sprey, T. (1984). The dorsal/ventral compartment boundary in Drosophila: coincidence with the prospective operculum seam. Wilehm. Roux. Arch. Dev. Biol. *193*, 133–138. https://doi.org/10.1007/BF00848888.

27. Spreij, T.E., and Segal, D. (1986). Determination of the shape of the operculum by the bithorax complex in Drosophila melanogaster. Roux's Arch. Dev. Biol. *195*, 318–322. https://doi.org/10.1007/BF00376064.

28. Kathirithamby, J. (1983). The mode of emergence of the adult male Elenchus.pdf. Zool. J. Linn. Soc. *77*, 97–102.

29. Lee, P.-T., Zirin, J., Kanca, O., Lin, W.-W., Schulze, K.L., Li-Kroeger, D., Tao, R., Devereaux, C., Hu, Y., Chung, V., et al. (2018). A gene-specific T2A-GAL4 library for Drosophila. Elife *7*, 135574. https://doi.org/10.7554/eLife.35574.

STAR★METHODS

KEY RESOURCES TABLE

REAGENT or RESOURCE	SOURCE	IDENTIFIER
Chemicals, peptides, and recombinant proteins		
Calcofluor White Stain	Biotium	Cat#29067
D-Glucose	Tokyo Chemical Industry	Cat#G0047
Nitro-Blue-Tetrazolium (NBT)	Sigma-Aldrich	N6876-50MG
Phenazine Methylsulfate (PMS)	Sigma-Aldrich	P9625-500<MG
VECTASHIELD	Vector Laboratories	H-1000-10
Experimental models: Organisms/strains		
D. melanogaster: w[1118]; P{NRE-EGFP.S}5A	Bloomington Drosophila Stock Center	RRID:BDSC_30727
D. melanogaster: P{UAS-Dcr-2.D}1, w[1118]; P{en2.4-GAL4}e16E, P{UAS-myr-mRFP}1, P{NRE-EGFP.S}5A	Bloomington Drosophila Stock Center	RRID:BDSC_30730
D. melanogaster: w[1118;] P{en2.4-GAL4}e16E, P{UAS-RFP.W}2/CyO	Bloomington Drosophila Stock Center	BDSC_30557
D. melanogaster: y[1] w[*]; P{Act5C-GAL4}25FO1/CyO, y+	Bloomington Drosophila Stock Center Kyoto Stock Center	RRID:BDSC_4414 RRID:DGGR_107727
D. melanogaster: w[1118]; P{GMR10G01-GAL4}attP2	Bloomington Drosophila Stock Center	RRID:BDSC_48270
D. melanogaster: y[1] w[*]; Mi{Trojan-GAL4.0}SerMI05334-TG4.0/TM3, Sb[1] Ser[1]	Bloomington Drosophila Stock Center	RRID:BDSC_78380
D. melanogaster: y[1] w[*]; Mi{Trojan-GAL4.1}DeltaMI04868-TG4.1/TM3, Sb[1] Ser[1]	Bloomington Drosophila Stock Center	RRID:BDSC_77753
D. melanogaster: y[1] sc[*] v[1] sev[21]; P{TRiP.GL00092}attP2	Bloomington Drosophila Stock Center NIG-FLY	RRID:BDSC_35213 GL00092
D. melanogaster: y[1] v[1]; P{TRiP.JF02959}attP2	Bloomington Drosophila Stock Center	RRID:BDSC_27988
D. melanogaster: y[1] v[1]; P{TRiP.JF03140}attP2	Bloomington Drosophila Stock Center	RRID:BDSC_28713
D. melanogaster: P{KK108416}VIE-260B	Vienna Drosophila Recource Center	V108348; RRID:Flybase_FBst0480159
D. melanogaster: y[1] v[1]; P{TRiP.JF02867}attP2	Bloomington Drosophila Stock Center	RRID:BDSC_28032
D. melanogaster: y[1] sc[*] v[1] sev[21]; P{TRiP.GL00520}attP40	Bloomington Drosophila Stock Center	RRID:BDSC_36784
D. melanogaster: P{KK103488}VIE-260B	Vienna Drosophila Recource Center	v108361; RRID:Flybase_FBst0480172
D. melanogaster: w[1118]; P{GD5611}v38041	Vienna Drosophila Recource Center	v38041; RRID:Flybase_FBst0462301
D. melanogaster: w[*]; P{UAS-Ser.mg5603}SS1	Bloomington Drosophila Stock Center Kyoto Stock Center	RRID:BDSC_5815 RRID:DGGR_108439
D. melanogaster: w[*]; sna[Sco]/CyO; P{UASt-Lifeact-RFP}3	Bloomington Drosophila Stock Center	RRID:BDSC_58362
D. melanogaster: w[*]; P{w[+mC] = UAS-GFP.S65T}e.g.,[T10]	Bloomington Drosophila Stock Center Kyoto Stock Center	RRID:BDSC_1522 RRID:DGGR_106364
D. melanogaster: y[1] w[1118]; PBac{y[+mDint2] w[+mC] = UAS-ChtVis-Tomato}VK00001	Bloomington Drosophila Stock Center	RRID:BDSC_66512
D. melanogaster: w[1118]; Gld[n1] p[p] cu[1]/TM6B, Tb[1]	Bloomington Drosophila Stock Center	RRID:BDSC_2440
D. melanogaster: Dfd[1] Gld[n2] p[p]/TM3, Sb[1]	Bloomington Drosophila Stock Center	RRID:BDSC_2439
D. melanogaster: y[1] N[l1N-ts1] g[2] f[1]/C(1)DX, y[1] f[1]	Bloomington Drosophila Stock Center Kyoto Stock Center	RRID:BDSC_2533 RRID:DGGR_107388
D. melanogaster: w[*] P{PTT-GA}Nrg[G00305]	Kyoto Stock Center	RRID:DGGR_110658
D. melanogaster: w[*]; Obst-E-a-GFP[F6]	Tajiri et al.[5]	N/A
D. melanogaster: w[*]; Obst-E-a-GFP[F11]	Tajiri et al.[5]	N/A
D. melanogaster: w[*]; Cpr11A-EGFP[6M]	Tajiri et al.[8]	N/A

(*Continued on next page*)

Continued		
REAGENT or RESOURCE	SOURCE	IDENTIFIER
D. melanogaster: w[*]; Cpr11A-EGFP[2M]	Tajiri et al.[8]	N/A
D. melanogaster: w[*]; Tb-GFP	gift from B. Moussian[7]	N/A
Software and algorithms		
ImageJ	NIH	https://imagej.net/ij/index.html

RESOURCE AVAILABILITY

Lead contact

Further information and requests for resources and reagents should be directed to and will be fulfilled by the lead contact, Tetsuya Kojima (tkojima@k.u-tokyo.ac.jp).

Materials availability

This study did not generate new unique reagents.

Data and code availability

This paper does not report original code. Any additional information required to reanalyze the data reported in this paper is available from the lead contact upon request.

EXPERIMENTAL MODEL AND SUBJECT DETAILS

Fly stocks and genetics

Flies were maintained on standard yeast-cornmeal food at 25°C unless otherwise mentioned. Both male and female flies were used, with essentially the same results. For examination of the chitin staining pattern and of the distribution of Tb-GFP, Cpr11A-EGFP, and Obst-E-a-GFP, late third instar larvae were used. For examination of the ChtVis-Tomato distribution, late third instar larvae and 4 hr and 72 hr APF pupae were used. Fly lines or alleles used were as follows: Canton-S (wild-type), *Act5C*-GAL4, *e22c*-GAL4, $Dl^{MI04868\text{-}TG4.1}$ (*Dl*-GAL4), *en*-$GAL4^{e16E}$, GMR10G01-GAL4, $NRE\text{-}EGFP^{5A}$, $Ser^{MI05334\text{-}TG4.0}$ (*Ser*-GAL4), UAS-$Dl^{JF02867}$ and UAS-$Dl^{GL00520}$ (*Dl*RNAi), UAS-$Gld^{v108361}$ and UAS-Gld^{v38041} (*Gld*RNAi), UAS-$Notch^{GL00092}$ and UAS-$Notch^{JF02959}$ (*Notch*RNAi), UAS-$Ser^{JF03140}$ and UAS-$Ser^{v108348}$ (*Ser*RNAi), UAS-Ser^{SS1} (*Ser* misexpression), UAS-$GFPS65T^{T10}$, UAS-$Lifeact\text{-}RFP^{3}$, UAS-$myr\text{-}mRFP^{1}$, UAS-$mRFP^{2}$, UAS-$ChtVis\text{-}Tomato^{VK00001}$, Gld^{n1}, Gld^{n2}, N^{ts1}, Nrg^{G00305} (*Nrg-GFP*), *Obst-E-a-GFP*, *Cpr11A-EGFP*, and *Tb-GFP*. $Dl^{MI04681\text{-}TG4.1}$ and $Ser^{MI05334\text{-}TG4.0}$ are protein-traps in which the T2A auto-cleaving sequence is inserted upstream of GAL4, and functional GAL4 is expressed under the control of the endogenous regulatory system in these lines.[29] Gld^{n1} and Gld^{n2} are strong hypomorphs[14] and were used as trans-heterozygotes. Fly stock sources are listed in the key resources table. Knockdown and ectopic expression were performed by crossing the appropriate GAL4 line and UAS flies. Detailed genotypes and conditions in each experiment are shown in Table S1. Especially, the localizations of Obst-E-a-GFP and Cpr11A-EGFP were observed in flies having two copies of constructs for wild-type and one copy for RNAi flies and *Gld* mutants. Tb-GFP localization was observed in flies having one copy of the construct in all experiments. ChtVis-Tomato signals were examined in flies with one copy each of *e22c*-GAL4 and UAS-*ChtVisTomato*. In the experiment using the temperature-sensitive allele of *Notch*, N^{ts1}, larvae shifted to 29°C from 18°C at the early second instar were observed at the late third instar.

METHOD DETAILS

Chitin staining

Chitin staining was performed as described previously.[5] In brief, the cuticle with epidermal cells was dissected from late third instar larvae in PBS [10 mM phosphate buffer (pH 7.2), 150 mM NaCl] and fixed in 4% paraformaldehyde in PBS for 10–30 min at room temperature. They were stained by 2 μg/ml Calcofluor White Stain in PBT (PBS containing 0.1% Triton X-100) for 1 hr at room temperature and washed in PBT three times at room temperature. After rinsing with PBS, specimens were mounted in VECTASHIELD (Vector Laboratories).

Gld activity staining

Gld activity staining was performed according to previously described methods.[19,25] In brief, the cuticle with epidermal cells was dissected as described above and washed in 200 mM Tris-HCl (pH 6.8). Samples were transferred to the Gld staining solution [200 mM Tris-HCl (pH 6.8), 120 mM D-Glucose, 1.1 mM Nitro-Blue-Tetrazolium (NBT), 0.157 mM Phenazine Methylsulfate (PMS)] and incubated for 15–30 min at room temperature in the dark. After signals were developed, specimens were washed in PBS and mounted in PBS.

Microscopy

Images of Gld staining were obtained using the stereomicroscope SZX-12 (OLYMPUS, Tokyo, Japan) equipped with the CCD camera VB-7010 (KEYENCE, Osaka, Japan) or BX51 (OLYMPUS) equipped with the Spot RT Slider camera (Diagnostic Instruments, Sterling Heights, MI, USA). For fluorescence signals, the stereomicroscope SZX-12 (OLYMPUS) equipped with the CCD camera VB-7010 (KEYENCE), or the confocal laser scanning microscope FV-1000 (OLYMPUS) or FV-3000 (OLYMPUS) was used. The super-resolution mode of FV-3000 was used to observe the fine, filamentous chitin staining signal and Obst-E-a-GFP localization. We were not able to analyze Cpr11A-EGFP and ChtVis-Tomato signals clearly by the super-resolution mode due to severe signal decay. Videos were taken using SZX-12 (OLYMPUS) equipped with the CCD camera VB-7010 (KEYENCE). For electron microscopic observations, dissected and fixed larval cuticles were sent to the Hanaichi UltraStructure Research Institute (Aichi, Japan) for observation.

Observation of ChitVis-Tomato signals in the pupal stage

Six pieces of vinyl tape with a square hole in the center were stacked and stuck to a glass slide. A pupa was placed in the hole, oriented lateral side up, and mounted in VECTASHIELD (Vector Laboratories). Samples were observed using the FV-1000 (OLYMPUS).

QUANTIFICATION AND STATISTICAL ANALYSIS

Nrg-GFP signals were traced, and cell area, circularity, and roundness were calculated using Image J. OR-forming cells and cells dorsally and ventrally touching OR-forming cells in the central region of T3 were analyzed. Total of 78 (dorsal cells), 50 (OR-forming cells), and 84 (ventral cells) cells from seven larvae were analyzed. Statistical analyses were performed in Microsoft Excel. Significance was evaluated using t-test with Bonferroni correction. Data used for calculation are provided in Table S2.